Experimental evidence of excited electron number density and temperature effects on electron-phonon coupling in gold films

Ashutosh Giri, John T. Gaskins, Brian M. Foley, Ramez Cheaito, and Patrick E. Hopkins

---

Articles you may be interested in

Ultrafast and steady-state laser heating effects on electron relaxation and phonon coupling mechanisms in thin gold films
Appl. Phys. Lett. **103**, 211910 (2013); 10.1063/1.4833415

Electron temperature dependence of the electron-phonon coupling strength in double-wall carbon nanotubes
Appl. Phys. Lett. **103**, 043110 (2013); 10.1063/1.4816055

Experiment study of the size effects on electron-phonon relaxation and electrical resistivity of polycrystalline thin gold films
J. Appl. Phys. **108**, 064308 (2010); 10.1063/1.3482006

Contribution of d -band electrons to ballistic transport and scattering during electron-phonon nonequilibrium in nanoscale Au films using an ab initio density of states
J. Appl. Phys. **106**, 053512 (2009); 10.1063/1.3211310

Effects of electron scattering at metal-nonmetal interfaces on electron-phonon equilibration in gold films
J. Appl. Phys. **105**, 023710 (2009); 10.1063/1.3068476
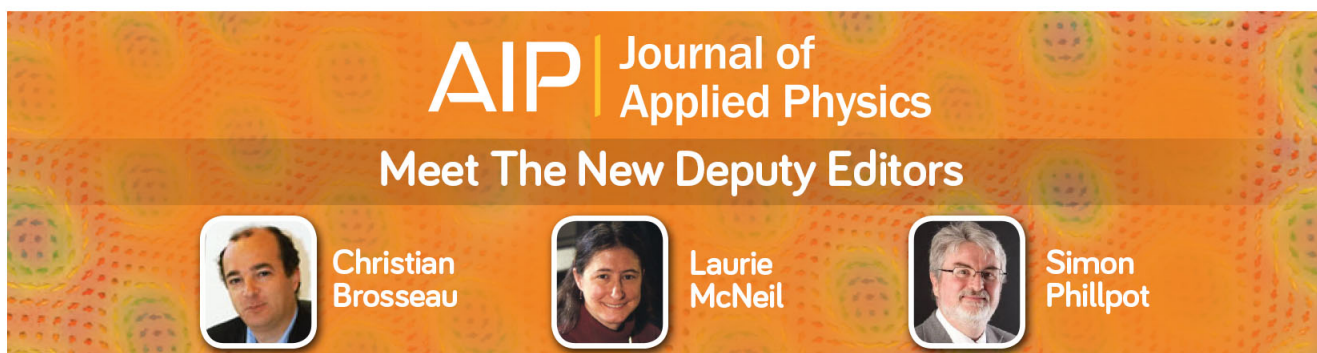
Experimental evidence of excited electron number density and temperature effects on electron-phonon coupling in gold films

Ashutosh Giri, John T. Gaskins, Brian M. Foley, Ramez Cheaito, and Patrick E. Hopkins[a)]
Department of Mechanical and Aerospace Engineering, University of Virginia, Charlottesville, Virginia 22904, USA

The electronic transport properties of metals with weak electron-phonon coupling can be influenced by non-thermal electrons. Relaxation processes involving non-thermal electrons competing with the thermalized electron system have led to inconsistencies in the understanding of how electrons scatter and relax with the less energetic lattice. Recent theoretical and computational works have shown that the rate of energy relaxation with the metallic lattice will change depending on the thermalization state of the electrons. Even though 20 years of experimental works have focused on understanding and isolating these electronic relaxation mechanisms with short pulsed irradiation, discrepancies between these existing works have not clearly answered the fundamental question of the competing effects between non-thermal and thermal electrons losing energy to the lattice. In this work, we demonstrate the ability to measure the electron relaxation for varying degrees of both electron-electron and electron-phonon thermalization. This series of measurements of electronic relaxation over a predicted effective electron temperature range up to ~3500 K and minimum lattice temperatures of 77 K validate recent computational and theoretical works that theorize how a nonequilibrium distribution of electrons transfers energy to the lattice. Utilizing this wide temperature range during pump-probe measurements of electron-phonon relaxation, we explain discrepancies in the past two decades of literature of electronic relaxation rates. We experimentally demonstrate that the electron-phonon coupling factor in gold increases with increasing lattice temperature and laser fluences. Specifically, we show that at low laser fluences corresponding to small electron perturbations, energy relaxation between electrons and phonons is mainly governed by non-thermal electrons, while at higher laser fluences, non-thermal electron scattering with the lattice is less influential on the energy relaxation mechanisms. © 2015 AIP Publishing LLC.
[http://dx.doi.org/10.1063/1.4906553]

I. INTRODUCTION

Understanding of the fundamental scattering processes that describe the interactions between electrons and lattice vibrations is significant to various phenomena in solid state physics such as superconductivity,[1] electronic and thermal transport,[2] spin caloritronics,[3,4] and laser induced phase transitions.[5–7] The substantial difference in the heat capacities between the electrons and the lattice allows for the selective perturbation and direct observation of scattering processes of the electron gas using short-pulsed lasers. Using time domain thermomodulation spectroscopy techniques, the energy relaxation and conversion processes between electronic and vibrational systems can be monitored in real time. The first observation of this nonequilibrium between the electronic and the vibrational states in metals with short-pulsed, time domain thermoreflectance (TDTR) was carried out by Eesley[8] who confirmed the earlier theories that were based upon the assumption of electrons and the lattice being described by two separate temperatures, which validated the two-temperature model (TTM).[9,10] Shortly after, femtosecond laser pulses were used to resolve the time taken by the electronic system to lose its energy to the lattice, allowing

for the measurement of electron phonon coupling constant, G, that quantifies the volumetric rate of energy transfer between the two states.[11–15] All of the aforementioned works were based on the assumption that the electrons thermalize within themselves on a time scale shorter than the laser pulse duration. However, photoemission measurements by Fann *et al.*[16,17] measured the thermalization time of the electron gas in gold as ~1 ps which is comparable to the electron-phonon (e-p) relaxation time.[11–15,18] Pump-probe femtosecond measurements have also demonstrated a long-living non-Fermi distribution of electrons in gold[19,20] on the order of the e-p relaxation time. This is in contrast to the theoretically calculated Fermi relaxation time of ~40 fs.[21] In fact, a recent computational study has shown that the thermalization time of the electron gas can span anywhere from 10 fs to picoseconds depending on the laser irradiation strength.[22]

The non-Fermi electron dynamics and the initial thermalization of the electron system influence the transient optical properties of thin metal films. For example, we have previously shown in Ref. 20 that not accounting for the delayed thermalization in the TTM leads to erroneous measurements of G. This built off of earlier work by Tas and Maris,[23] who questioned the validity of the classical TTM based on the fact that e-p collisions cause a significant change in the electron distribution as early as a few tens of

a)Electronic mail: phopkins@virginia.edu

117, 044305-1

femtoseconds after pulse absorption when the electron gas has not fully thermalized. They calculated the rate of energy transfer from the electron system to the lattice and showed that there is a significant difference between the fully thermalized electron system and when non-thermal electrons are accounted for in their calculations. Indeed, not accounting for non-thermal electrons in the prediction of the relaxation time between the two states produces an erroneously high rate of energy relaxation below room temperature for low electron perturbations[18,24] (we define the low perturbation limit as, $T_{e,eff} - T_p \ll T_p$, where $T_{e,eff}$ and T_p are the effective electron and phonon temperatures, respectively. We define the electron temperature as an "effective" temperature due to the fact that the time taken by the electron gas to relax to a Fermi distribution has been shown to be in the order of the e-p relaxation time). Recent work by Wang and Cahill[25] showed that for a fully thermalized electron system at low e-p nonequilibrium, the experimentally determined e-p coupling factor for Au and Cu is well predicted by the classical TTM. However, in the case of relatively high absorbed laser fluences and large e-p non-equilibrium, the effect of electron-electron (e-e) thermalization on the e-p coupling has not been rigorously studied. This has created a disconnect among over 20 years of literature that have experimentally studied the dynamics of e-p coupling during e-p nonequilibrium. Consequently, the behavior of non-thermal electron-phonon interactions during high energy, short-pulsed laser heating experiments is not well quantified.

In response, we investigate the e-e interaction dynamics that influence the e-p relaxation by probing the electron relaxation in thin gold films over a wide range of lattice temperatures (77–300 K) and absorbed laser fluences using TDTR.[26–28] Due to gold's weak electron-lattice interaction strength, relatively long Fermi-relaxation time, well characterized band structures, and extensively studied thermal properties and transport dynamics, gold represents an ideal platform to measure the e-p relaxation mechanisms at large laser perturbations and high electron temperatures. We show that the e-p coupling factor increases with electron temperature, which is in contrast to Kaganov's original theory[9] but qualitatively in line with a recent modification to Kaganov's theory.[29] Furthermore, we show a nearly linear dependence of the electron relaxation rate with an increase in lattice temperature for the low perturbation limit of the electron system. However, for high fluences and larger degrees of e-p nonequilibrium, the lattice temperature dependence on G becomes much less pronounced and is nearly constant for the largest fluences considered in this study. We use a modified version of the TTM to analyze our data that can account for a delay in the thermalization of the electrons. Our data demonstrate that the differences in measurements of e-p relaxation over the past 20 years can be explained by considering electron thermalization and e-e scattering.

II. EXPERIMENTAL DETAILS

A. Experimental technique and data analysis

Nominally, 20 nm of gold films was evaporated onto crystalline silicon substrates using electron-beam evaporation.

The electron-phonon relaxation mechanisms intrinsic to the sample were measured via a two-wavelength pump-probe technique where the pump pulses have been frequency doubled from 1.55 to 3.1 eV. We measured the FWHM of the probe pulse to be 220 ± 20 fs via the frequency resolved optical gating technique.[30] The cross correlation between the pump and the probe pulses was measured as 780 ± 20 fs. The $1/e^2$ radii of the pump and probe spot sizes after being focused through a $20\times$ objective were 6.5 and $6\,\mu m$, respectively, which was measured with a Scanning Slit Optical Beam Profiler. We conduct TDTR measurements from 77 to 296 K of sample (lattice) temperatures in an optical cryostat that maintains the pressure below 10^{-5} Torr.

The probe energy is below the interband transition threshold for Au (2.4 eV)[31] and the energy in the absorbed fluence from the pump pulses does not significantly change the conduction band number density from d-band excitations. In fact, we estimate that even with our maximum absorbed laser fluence (10.7 J m^{-2}), the conduction band number density will only be perturbed by $<2\%$ (Ref. 32) allowing for the use of the Drude-based thermoreflectance model,[33] the details of which are discussed below. The absorption of the pump pulses by the sample surface leads to a rapid increase in the internal energy of the electron system, which then transfers its energy to the lattice vibrations. This provides a unique path forward to directly measure how electrons in various states of nonequilibrium interact with the surrounding lattice. The change in the optical properties created by these relaxation processes is monitored with the reflected probe beam at the frequency with which we modulate the pump beam in our experiment (8.8 MHz).

The temperature dynamics underlying the measured thermoreflectance data were determined using a modified TTM.[20,34] The coupled partial differential equations in the TTM (Eq. 1) are derived under the assumption that the classical Fourier law can describe the energy transport of the carriers. In other words, the TTM is valid as long as the spatial and temporal characteristics of the temperature fields are greater than the mean free path and relaxation time of the energy carriers, respectively. However, due to the fact that the finite amount of time taken by the electron gas to relax to a Fermi distribution ($\sim$1 ps (Refs. 16 and 22)) is longer than the pulse duration used in our experiments, our modified TTM measures the "effective" electron temperatures from the time of pump absorption at the metal surface to the time taken by the electrons to fully thermalize within themselves and the metal lattice. Therefore, compared to the traditional TTM, the main aspect of the modified TTM is its ability to account for a temporally lagging evolution of the electron energy density after pulse absorption. The respective time evolution of the electron and lattice (phonon) temperatures are given by

$$C_e(T_{e,eff})\frac{\partial T_{e,eff}}{\partial t} = \nabla \cdot (\kappa_e \nabla T_{e,eff}) - G_{eff}(T_{e,eff} - T_p) + S(t),$$

$$C_p(T_p)\frac{\partial T_p}{\partial t} = \nabla \cdot (\kappa_p \nabla T_p) + G_{eff}(T_{e,eff} - T_p), \quad (1)$$

where C_e and C_p are the heat capacities of the electrons and phonons, respectively. Similarly, κ_e and κ_p are the thermal

conductivities of the electrons and phonons, respectively, and $S(t)$ is the source term which is modified to account for the delayed relaxation in the electronic distribution and is given as

$$S(t) = \frac{0.94F(1-R)}{d(t_p + t_{th})} \exp\left[-2.77\left(\frac{t - 2(t_p + t_{th})}{t_p + t_{th}}\right)^2\right], \quad (2)$$

where F is the laser fluence incident on the sample surface, R is the reflectivity of the sample, d is the film thickness, t_p is the pulse width, and t_{th} is the electron-electron thermalization time required for the majority of the electron gas to relax to a Fermi distribution after pulse absorption and is treated as a free parameter in the source term. The amount of laser energy absorbed in the sample is calculated based on the thin-film optics in Ref. 35 (note, we have verified these calculations for Au films in our earlier work).[34] Initially after laser pulse absorption, the non-Fermi distribution of electrons absorbs the photon energies and traverse the Au film thickness with velocities close to the Fermi velocity.[36] The electron diffusion term in the TTM can be neglected due to this ballistic nature of the "hot" electrons, which creates a homogeneously heated thin film within a few tens of femtoseconds. Also, the time scale considered in this work presents the simplification of not accounting for the phonon thermal diffusion. The coefficient of electronic heat capacity is taken from Ref. 37 and the lattice heat capacities at different temperatures are taken from Ref. 38. Since the phonon heat capacities at the temperatures studied in this work are more than an order of magnitude larger than that for the electrons, the phonon distribution changes are negligible in the femtosecond time scale.[39] For this reason, phonons can be described by a Bose-Einstein distribution and a temperature, T_p, which affects the electron dynamics at the picosecond time regime and dictates the final equilibrium temperature of the coupled subsystems.

For films that are thicker than the ballistic penetration depth of the electrons, the source term has to account for the depth of electronic thermalization.[36] However, due to the fact that our film thickness is smaller than the ballistic penetration depth in Au, the spatial resolution in the traditional source term can be safely neglected. Furthermore, the traditional source term in the TTM assumes that after pump pulse absorption, the electron system is fully thermalized and the peak reflectance would occur immediately after pump pulse absorption ($\sim$300 fs) as that would correspond to the maximum electron temperature. This is clearly not the case as the rise time of the fast transient for the TDTR measurements is $\sim$2 ps (Fig. 1), signifying a delay in the thermalization of the electron gas. Therefore, we add t_{th} in the source term to effectively account for nonthermal electron dynamics during that period. It is important to note that the predicted effective electron temperature in our experiments, $T_{e,eff}$, which we predict from our modified TTM analysis, does not exceed 3500 K. Above this temperature and corresponding electron energy density, the conduction band number density of electrons will be significantly increased due to thermal excitations from the d-band electrons in Au.[40] This also validates
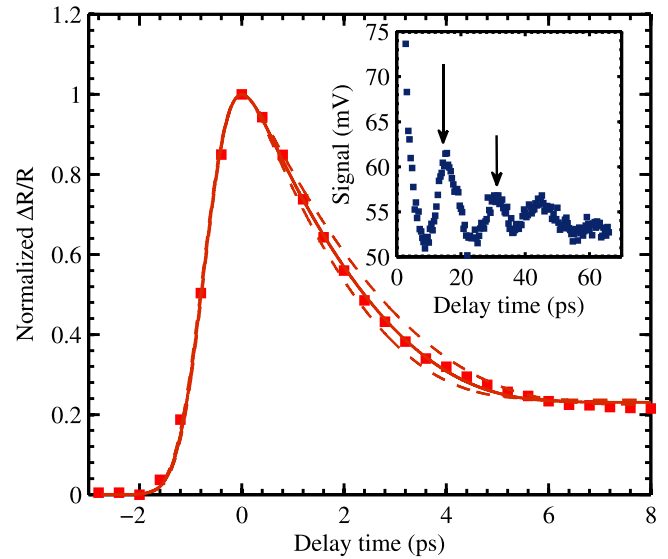

FIG. 1. TDTR signal on 26 nm Au/Si sample at an absorbed laser fluence of $F = 3.52$ J m^{-2} and corresponding best fit using the modified TTM with a nonlinear thermoreflectance model. The data are normalized by the maximum magnitude of the signal from the lock-in amplifier. The predicted maximum effective electron temperature in this data is 1750 K. (Inset) Picosecond acoustic response of the film used to measure the thickness. The technique relies on the oscillatory change in the thermoreflectance signal due to the propagation of strain wave caused by the sudden heating of the film. The round-trip time of the echo can be observed in the oscillatory signal (marked by the two arrows) and the thickness can be determined by correlating it to the longitudinal speed of sound in the gold film.

our use of a linear electron heat capacity as a function of electron temperature for the range of laser fluences used in this work.

B. Thermoreflectance model

In the thermoreflectance model, the change in the base line reflectivity of a sample surface is related to the change in the temperature predicted by the modified TTM at a particular laser fluence. The change in reflectance of a metal can be related to the change in temperature through the change in the complex dielectric function. For ultra-short pulses with t_p less than the e-p thermaliztion time, the dielectric function depends on changes in both the electron and phonon temperatures. For small perturbations in temperature ($\Delta T \sim 150$ K), corresponding low laser fluences, the change in reflectivity measured can be directly related to changes in electron and phonon temperatures through[14,41]

$$\frac{\Delta R}{R} = a\Delta T_e + b\Delta T_p, \quad (3)$$

where $a \propto \partial R / \partial T_e$ and $b \propto \partial R / \partial T_p$ and are usually determined by fitting predicted changes in temperature from the TTM. The validity of Eq. (3) breaks down at elevated temperatures (corresponding to high laser fluences) as the relation between temperature and reflectivity due to intraband transitions is highly nonlinear.[33] Smith and Norris[41] developed a thermoreflectance model that expands the temperature range applicable to measure thermophysical properties by exploiting the relationship between the metal's reflectivity and the change in the dielectric function due to changes

in electron and phonon temperatures. However, the complex dielectric function combines the effects due to interband transitions (free electrons) and intraband transitions (bound electrons), $\hat{\varepsilon} = \hat{\varepsilon}_{intra} + \hat{\varepsilon}_{inter}$. Since we are examining Au with 800 nm pulses (1.55 eV), we only need to consider intraband transitions as the lowest energy *d*-band to available *s*-band transition is very large for Au (2.4 eV).

The intraband part, $\hat{\varepsilon}_{intra}$, is described by the well-known Drude model[42,43]

$$\hat{\varepsilon}_{intra} = 1 - \frac{\omega_p^2}{\omega\left(\omega + i\tau_f^{-1}\right)}, \tag{4}$$

where ω is the angular frequency of the absorbed radiation, ω_p is the plasma angular frequency of the film, and τ_f^{-1} is the scattering rate of the free electrons undergoing intraband transitions. The temperature dependence in Eq. (4) comes from the scattering rate of these free electrons and can be estimated through the Matthiessen's rule,[44] $\tau_f^{-1} = A_{ee}T_{ee}^2 + B_{ep}T_p$, where A_{ee} and B_{ep} are constant coefficients relating to the temperature dependencies of electron-electron and electron-phonon collisional frequencies, respectively. The thermoreflectance model requires the proper knowledge of these scattering coefficients and in our earlier work,[34] we have shown that by replacing G in the TTM with G_{eff} (that is derived in Ref. 29) and fitting for the scattering coefficients in the regime of low electron perturbation, we can predict the values for A_{ee} and B_{ep}. For the thin Au film used in this work, the predicted scattering coefficients were $A_{ee} = 1.1 \times 10^7\,\mathrm{K^{-2}\,s^{-1}}$ and $B_{ep} = 1.3 \times 10^{-11}\,\mathrm{K^{-1}\,s^{-1}}$, in excellent agreement with the low temperature resistivity data[45] and literature values.[46]

The reflectivity of a bulk material at the air (vaccum)/film interface is given by

$$R = \frac{(n-1)^2 + k^2}{(n+1)^2 + k^2}, \tag{5}$$

where n and k are the real (refractive index) and imaginary (extinction coefficient) parts of the complex index of refraction. The intraband part of the optical dielectric function, $\hat{\varepsilon}_{intra} = \varepsilon_1 + i\varepsilon_2$, is further related to the refractive index and extinction coefficient through[43]

$$n = \frac{1}{\sqrt{2}}\left[\left(\varepsilon_1^2 + \varepsilon_2^2\right)^{1/2} + \varepsilon_1\right]^{1/2} \tag{6}$$

and

$$k = \frac{1}{\sqrt{2}}\left[\left(\varepsilon_1^2 + \varepsilon_2^2\right)^{1/2} - \varepsilon_1\right]^{1/2}. \tag{7}$$

Equation (5) does not account for multiple reflections and absorptions at the film/substrate interface for thin films that are in the order of the optical penetration depth. As the Au film under study is optically thin at 800 nm, we use thin film optics, to calculate the reflectivity for a thin film on a substrate where the incident medium is air,

$$R_f = r^*r, \tag{8}$$

where

$$r = \frac{(m_{11} + \hat{n}_s m_{12}) - (m_{21} + \hat{n}_s m_{22})}{(m_{11} + \hat{n}_s m_{12}) + (m_{21} + \hat{n}_s m_{22})} \tag{9}$$

with $\hat{n}_s$ being the complex index of refraction of the substrate ($\hat{n}_s = n_s + ik_s$) and r^* is the complex conjugate of Eq. (9). m_{ij} is the component of the characteristic thin film matrix defined as

$$m_{ij} = \begin{bmatrix} \cos\delta & -\dfrac{i}{\hat{n}_f}\sin\delta \\ -i\hat{n}_f\sin\delta & \cos\delta \end{bmatrix}, \tag{10}$$

where $\delta = \omega d\hat{n}_f/c$ and c is the speed of light and d is the film thickness. Once Eq. (9) is determined, the final change in reflectivity due to temperature changes of the film/substrate system is given by

$$\frac{\Delta R}{R} = \frac{R_f(T_{e,eff}) - R_f(T_0)}{R_f(T_0)}, \tag{11}$$

where T_0 is the ambient temperature.

A typical TDTR signal is shown in Fig. 1 (red square) along with the solid line that represents the fit to the data set with the modified TTM in conjunction with the thermoreflectance model. The dashed lines represent fits for values of G_{eff} that include the standard deviation in the experimental data. The main sources of error in the experiment are the measurement of the laser spot sizes, determination of the thickness of the sample, and the repeatability of the measurements. The thickness of the 26 nm Au film is confirmed via picosecond acoustics[47] (Fig. 1 inset; note, precise knowledge of this film thickness is imperative for proper prediction of the electron energy density during and after pulse absorption) as is apparent from calculations of thin film matrix in Eq. (10) and the source term in Eq. (2).

III. RESULTS AND DISCUSSION

Fig. 2 shows the measured effective electron-phonon coupling, G_{eff}, that considers the energy transfer from both the thermal and non-thermal distribution of electrons, as a function of lattice temperature for two different absorbed laser fluences (blue squares represent $F = 0.1\,\mathrm{J\,m^{-2}}$ and red circles represent $F = 3.52\,\mathrm{J\,m^{-2}}$). Also plotted are the G_{eff} values calculated from the experimental e-p relaxation times at different temperatures from Ref. 18 (hollow squares). The laser fluence in their study is comparable to the lowest absorbed laser fluence used in this work, and their G_{eff} agree very well with our measured values using our modified TTM approach. At these low electron perturbations, there is a linear increase in G_{eff} with an increase in lattice temperature. For low fluences, the e-p coupling factor can be estimated as, $G_{eff} = \gamma T_p/\tau_E$, where τ_E is the e-p relaxation time. There is a slow decrease in τ_E as the temperature is lowered from 300 K to 77 K, therefore the effective e-p coupling factor scales with the lattice temperature at these low excitation regimes. On the other hand, the higher fluence data agree with the classical TTM which describes the energy transfer
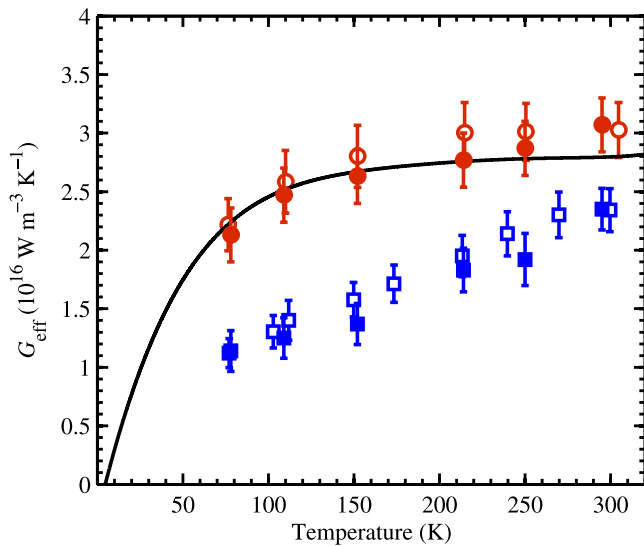
FIG. 2. G_{eff} as a function of lattice temperature for two different fluences. At a higher fluence resulting in an increase in peak electron temperature, the electron system couples more readily with the lattice. At these temperatures, the data match with the classical TTM (solid line) which does not account for non-thermal electrons in the model and also match with data from Ref. 25 which is characterized by an electron system that is fully thermalized. The low fluence data match the experimental data from Ref. 18 and confirm that at low electron perturbations, the non-thermal electrons significantly reduce the e-p coupling in gold with a larger contribution from these non-thermal electrons at lower lattice temperatures.

rate as $H(T_{\mathrm{e,eff}}, T_{\mathrm{p}}) = f(T_{\mathrm{e,eff}}) - f(T_{\mathrm{p}})$, where $f(T)$ is given as[9]

$$f(T) = 4G_0 \left(\frac{T}{\theta_D} \right)^5 \int_0^{\theta_D/T} \frac{x^4}{e^x - 1} dx. \qquad (12)$$

Here, θ_D is the Debye temperature of Au (170 K) and G_0 is the e-p coupling constant for the high temperature limit ($T \gg \theta_D$). Note that the classical TTM does not account for the non-thermal electrons that lose energy to the surrounding environment and only sums all the one-phonon emission and absorption processes for the case of a thermalized electron gas. The high fluence data in Fig. 2 also agree with the experimental data from Ref. 25 (hollow circles) which reports G of a gold film under conditions of a nearly fully thermalized electron system. The reason for our agreement with the classical TTM and data from Ref. 25 is discussed in detail in the remainder of this work, focusing on the interplay between thermal and nonthermal electrons.

The observations from Fig. 2 are in line with recent computational work by Mueller and Rethfeld.[22] Their work demonstrated that at low electron temperatures, the electron thermalization is slower and the non-thermal electrons interact with the lattice at a slower rate (up to $T_{\mathrm{e}} \sim 3000$ K) compared to electrons in an equilibrium distribution. At low effective electron temperatures, which corresponds to low absorbed fluences, the population of non-thermal electrons is larger than at higher effective electron temperatures, resulting in lower G than the thermalized limit. This can also be understood in terms of Landau's Fermi liquid theory, in which the quasiparticles (electrons and holes) have an average lifetime that is inversely proportional to the energy of

the quasiparticles.[48] The non-thermal distribution of quasiparticles lose their energy by colliding with particles in the Fermi sea, distributing roughly half of their energy to the electrons in the Fermi level. By doing so, the number of excitations double and increase the rate of energy exchange with the lattice. At low laser fluences, the e-e thermalization process is much slower compared to the high absorbed fluence case due to lower number of excitations in the limited phase space to which the electrons can scatter.[22] This explains the reduced G_{eff} for the case of low electron perturbations. As a result, at these low $T_{\mathrm{e,eff}}$, when the thermalization time of the electron gas is comparably longer,[22] the experimental data (solid blue and unfilled blue squares) do not agree with the classical TTM, mainly because of non-thermal electrons losing energy to the lattice at a slower rate as discussed above. This observation is consistent with Mueller and Rethfeld's[22] work where at low $T_{\mathrm{e,eff}}$, the e-p coupling factor for non-thermalized electrons is very low. However, at a higher fluence due to shorter thermalization time and lesser effect from the non-thermal electrons, our data (solid red circles) agree very well with Kaganov's TTM and the experimental data from Wang and Cahill[25] (hollow red circles). They measure G when the electrons have fully thermalized and the effect due to non-thermal electrons is minimal. We note that in our experimental setup with a $1/e^2$ radius of 6.5 μm pump spot size, there is a 7 fold change in laser intensity (from center to $1/e^2$ radius of Gaussian distribution), which initially excites a range of electronic states within this region. For a laser wavelength of 800 nm, and a final electron temperature, $T_{\mathrm{e}} < 1000$ K, the thermalization time is >1 ps whereas, for a final electron temperature of $T_{\mathrm{e}} \sim 3000$ K, the thermalization time is <100 fs (calculated by solving the Boltzmann transport equation with the relaxation time approximation).[22] Therefore, the thermalization time for the electrons excited by the pump pulse will depend on the radial distance from the center of the laser spot. The majority of the nonthermal electrons that influence our experiment after the peak in the TDTR signal where we determine G_{eff} are contained in the tail end of the Gaussian, which are consistent with the fluence that we assume in our calculations. To this end, our pump and probe spot sizes are very similar and the absorbed fluence calculated in this work denotes an average absorbed fluence in the region of space defined by the $1/e^2$ radius of the probe pulse, which, due to the similar spot sizes of the pump and probe, also correctly reflects the total absorbed energy by the pump. However, if the pump spot were much larger than the probe spot, then the probe will only sample a small portion of the pump heating event, and the sampling in the probe will not reflect the entire absorbed fluence in the pump. To this end, we have repeated our measurements of G_{eff} in our sample only now using a $5\times$ objective as opposed to a $20\times$ objective. This substantially increased the pump spot relative to the probe spot and resulted in $1/e^2$ radii of the pump and probe spot sizes of 42 μm and 10 μm, respectively. The thermoreflectance data were measured with a pump power of 100 mW, which results in an average fluence of the pump beam in the radius of the probe to be 1.5 J m^{-2} (which we calculate based on the intensity distribution of the pump spot, but only

considering the intensity distribution in a $10\,\mu m$ radius around the center of the Gaussian). Using our TTM to analyze the data, we measure $G_{eff} = 2.9 \times 10^{16}\,\mathrm{W\,m^{-3}\,K^{-1}}$ for $T_{e,eff} \sim 1200\,\mathrm{K}$ at room temperature. This result agrees with the effective e-p coupling factor measured with similar pump and probe spot sizes. However, repeating our analysis above only now using the average fluence calculated based on the pump radius of $42\,\mu m$ in the TTM, we measure $G_{eff} = 1.8 \times 10^{16}\,\mathrm{W\,m^{-3}\,K^{-1}}$ for $T_{e,eff} \sim 500\,\mathrm{K}$. This result does not agree with our results nor previous measurements of e-p coupling factor[18,25] at these electron and phonon temperatures. Therefore, care must be taken in calculating the average fluence when using different pump and probe spot sizes.

The combined effect of e-e and e-p collisions on the rate of energy transfer to the lattice was calculated by Tas and Maris.[23] They showed that if only e-p interactions are considered, then the electrons would monotonically lose energy to the lattice; however, when e-e scattering plays a role, the rate of energy transfer to the lattice increases as the electrons thermalize. Therefore, the energy relaxation rate $(G_{eff}T_{e,eff})$ to the lattice increases as the thermalization process of the electron gas progresses, evident from the slow rise of the thermoreflectance response shown in Fig. 1. In Fig. 3(a), we have plotted the calculated rate of energy loss from the electrons to the lattice $(\dot{Q})$ as a function of time. The dotted line is calculated from the classical TTM which fails to reproduce the slow rise of the thermoreflectance signal. The solid line represents the calculations from our modified TTM which captures the increasing rate of energy exchange to the lattice due to the initial thermalization of the electron gas driven by the combined effect of e-e and e-p scattering.[23] Therefore, at low absorbed laser fluences, the non-thermal electrons contribute considerably to G_{eff} due to a slower rate of e-e

scattering and the classical TTM fails to predict the e-p energy relaxation time, τ_E, below room temperature at these low electron perturbations.[18]

We compare our experimental τ_E to the predictions from our modified TTM for various lattice temperatures in Fig. 3(b). The calculated instantaneous relaxation time is given by the expression[18]

$$\tau_E = \frac{\gamma\left(T_{e,eff}^2(0) - T_p^2\right)}{2G_{eff}\left(T_{e,eff}(0) - T_p\right)}, \tag{13}$$

where γ is the coefficient of electronic heat capacity. Where the classical TTM (solid line) fails to predict the experimental τ_E, the modified TTM is able to accurately predict the relaxation times, further solidifying our claim that the non-thermal electron dynamics have to be accounted for in the TTM to accurately measure G_{eff}. We note that this approach of using a modified TTM to extract electron-phonon relaxation dynamics from TDTR data has far less assumptions and fitting parameters than previous works using a full Boltzmann Transport Equation approach.[24,49]

In Fig. 4(a), we plot G_{eff} for different laser fluences as a function of the baseline lattice temperature before pulse excitation, T_p. Since the gold film is on a silicon substrate, the steady-state temperature perturbation due to laser heating can be neglected,[26,34] and we take the baseline lattice temperature as the temperature of the sample holder in the cryostat to which our sample is affixed. The maximum $T_{e,eff}$ at $T_p = 78\,\mathrm{K}$ and $300\,\mathrm{K}$ for the different laser fluences are also reported in Fig. 4(a). As the maximum $T_{e,eff}$ increases with the absorbed laser fluence, the electrons lose energy much more readily to the lattice for a given T_p. This is mainly due to the Pauli exclusion principle which in effect only allows electrons in a small interval of energy ($\approx k_B T_{e,eff}$) around the Fermi level to take part in the e-p collisions. The increase in $T_{e,eff}$ broadens this energy interval and increases the number of electronic states that lose energy to the vibrational states.

The trend in the increase in G_{eff} at various T_p changes with increasing fluences. At the lowest fluence, the trend is linear and the maximum $T_{e,eff}$ at a certain T_p increases as lattice temperature increases as discussed above. However, at higher fluences, this is not the case and the maximum $T_{e,eff}$ for a given fluence is at the lowest lattice temperature (77 K). At these high excitation regimes ($T_{e,eff} - T_p \gg T_p$), the instantaneous relaxation time can be estimated as $\tau_E \approx T_{e,eff}\gamma/G_{eff}$ and therefore the e-p relaxation does not scale with the lattice temperature for these fluences.

To understand the competing effects between electrons in equilibrium and non-equilibrium conditions, we replot the data from Fig. 4(a) along with recent theoretical results as a function of maximum $T_{e,eff}$. The results from the work by Lin *et al.*[40] consider electrons in a thermalized state within themselves whereas, the results from Mueller and Rethfeld[22] only consider electrons in a fully nonequilibrium state. Discrepancies between the theoretical models and the experimental data are due to the fact that our data include effects due to some combination of non-thermal and thermal populations of electrons during and after laser irradiation. At
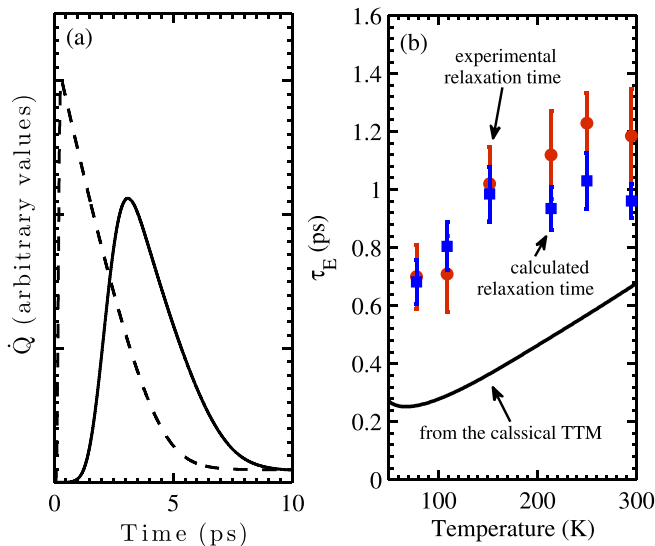

FIG. 3. (a) Rate of energy loss from the electrons to the lattice as a function of time after the laser pulse absorption. The solid line represents calculated $\dot{Q}$ with the modified TTM, whereas the dotted line is the profile calculated with the classical TTM. (b) Electron-phonon relaxation time as a function of lattice temperature. The accuracy of the modified TTM can be evaluated by comparing the calculated relaxation time and the experimental relaxation time in the case of the modified TTM and the classical TTM (solid line).
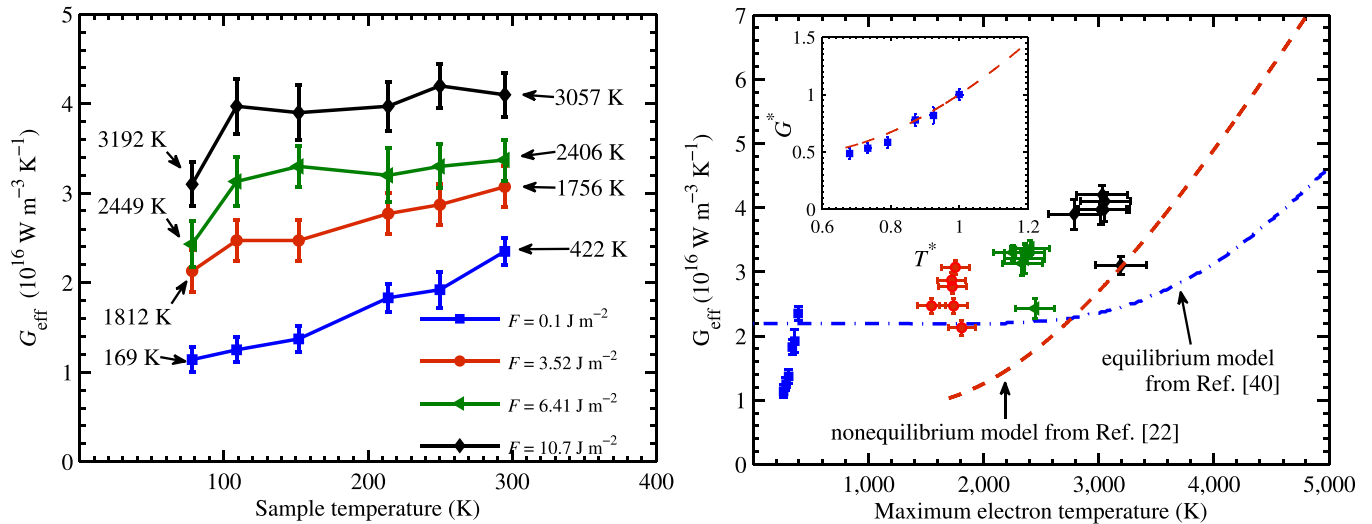
FIG. 4. (a) G_{eff} as a function of lattice temperature for four different fluences with the corresponding maximum $T_{e,eff}$ for 77 K and 300 K. (b) G_{eff} as a function of maximum $T_{e,eff}$ for different fluences with comparison to theoretical results from Lin *et al.*[40] (which considers the electrons in a thermalized state within themselves) and Mueller *et al.*[22] (which considers electrons in a non-thermalized state within themselves). (Inset) G_{eff} for the lowest fluence case having the maximum influence due to non-thermal electrons, normalized by the room temperature value at that fluence and plotted as a function of normalized temperature ($T_{e,eff}$ normalized by the room temperature value of $T_{e,eff}$ at that fluence). The dashed line represents the theoretical model under non-equilibrium condition, normalized by the room temperature value of G_{eff} for the lowest fluence case. The agreement between the data and the model suggests that at these fluences, e-p coupling is dominated by non-thermal electrons.

higher electron temperatures, the effects due to non-thermal electrons are significantly reduced and the increase in the data is much less pronounced compared to the strong increase in the low excitation regime.

The inset to Fig. 4(b) compares the non-equilibrium model from Ref. 22 with our experimental data for the lowest fluence case which demonstrates the maximum influence due to non-thermal electrons. Direct comparison of the non-thermal model to our experimental data for the lowest absorbed laser fluence case cannot be made because the data reported in Ref. 22 are limited to high electron temperatures ($T_e > 1800$ K), whereas the electron temperatures predicted by our experimental data are in the range of 160–430 K. However, to compare the characteristic trends involved with non-thermal population of electrons relaxing with the lattice, we normalize the data with the value for the e-p coupling constant predicted for the fully thermalized system at 0 K in Ref. 40. We normalize the nonthermal model (Ref. 22) at the electron temperature where the e-p coupling factor predicted for the model equals G of the fully thermalized system predicted in Ref. 40. This allows us to compare the trends between the nonthermal model and our experimental data. The nonthermal model predicts the trend in the experimental data very well, signifying that at these low fluences, non-equilibrium electrons dominate the e-p relaxation mechanism. The constant e-p coupling factor predicted by the classical TTM for temperatures greater than the Debye temperature cannot predict the increasing quasi-linear trend in the data at higher temperatures.

In an earlier work,[34] we have shown that Chen's model[29] for the e-p coupling factor can adequately predict this behavior. This model, which considers a thermalized electron system interacting with both itself and the lattice, should be valid at high enough fluences as the electron relaxation time decreases considerably and the effect due to

non-thermal electrons is minimized. However, due to the presence of non-thermal population of electrons in our data even at the maximum absorbed fluence of 10.7 J m^{-2}, there is still notable discrepancy between the model and the data at these high excitation regimes.

It should be noted that in Ref. 34, we provide evidence of adiabatic conditions between metal electrons and substrate phonons for a thermalized electron system. Thin gold films deposited on glass and Si substrates showed similar results for G_{eff} at various electron temperatures, alluding to the fact that there does not exist a direct energy coupling channel between the metal-electrons and the nonmetal-phonons. We attribute this to the weak adhesion between the film and the substrate and also to the potential barrier created for the electrons near the interface. However, it has been shown that at relatively high non-equilibrium conditions, electron to substrate energy coupling could represent a unique pathway to enhance heat flow across interfaces.[34,50–53] We are currently experimentally investigating the thermal boundary conductance driven by metal electrons directly interacting with the nonmetal phonons in detail.

IV. SUMMARY

In summary, we have measured the effective e-p coupling factor of Au from lattice temperatures, 77–300 K. We account for the non-thermal electrons that lose energy to the lattice with our modified TTM approach that we use to back out the respective temperatures for the electronic and vibrational states. We experimentally show that these non-thermal processes significantly alter the coupling mechanism between the two carriers. Specifically, at low electron perturbations, the delay in the thermalization process results in a suppressed e-p coupling and the energy relaxation mechanism scales with the lattice temperature. At higher fluences

and higher excitation regimes, due to faster thermalization of the electron gas, the effect due to non-thermal population of electrons is significantly reduced and the increase in the number of excitations leads to faster coupling between the two states.

While it has been shown that electron relaxation processes are dependent on the lattice temperature, conventional pump-probe experiments have not been able to accurately pin point the variation of over 20 years of reported values of the electron-phonon coupling factor at low lattice temperatures ($T_\mathrm{p} < 300\,\mathrm{K}$). Our work considers varying laser fluences at a range of sample temperatures, which allows the comprehensive study of varying degrees of electron-electron and electron-phonon nonequilibrium that have only been studied computationally.

ACKNOWLEDGMENTS

[1]P. B. Allen, Phys. Rev. Lett. **59**, 1460 (1987).
[2]G. Grimvall, *Selected Topics in Solid State Physics*, edited by E. Whohlfarth (North-Holland, New York, 1981).
[3]J. Sinova, Nature Mater. **9**, 880 (2010).
[4]G. E. W. Bauer, E. Saitoh, and B. J. van Wees, Nature Mater. **11**, 391 (2012).
[5]W.-L. Chan, R. S. Averback, D. G. Cahill, and A. Lagoutchev, Phys. Rev. B **78**, 214107 (2008).
[6]D. S. Ivanov and L. V. Zhigilei, Phys. Rev. B **68**, 064114 (2003).
[7]W.-L. Chan, R. S. Averback, D. G. Cahill, and Y. Ashkenazy, Phys. Rev. Lett. **102**, 095701 (2009).
[8]G. L. Eesley, Phys. Rev. Lett. **51**, 2140 (1983).
[9]M. Kaganov, I. Lifshitz, and L. V. Tanatarov, Sov. Phys. JETP **4**, 173 (1957).
[10]S. I. Anisimov, B. L. Kapeliovich, and T. L. Perelman, Sov. Phys. JETP **39**, 375 (1974).
[11]H. E. Elsayed-Ali, T. B. Norris, M. A. Pessot, and G. A. Mourou, Phys. Rev. Lett. **58**, 1212 (1987).
[12]R. W. Schoenlein, W. Z. Lin, J. G. Fujimoto, and G. L. Eesley, Phys. Rev. Lett. **58**, 1680 (1987).
[13]S. D. Brorson, J. G. Fujimoto, and E. P. Ippen, Phys. Rev. Lett. **59**, 1962 (1987).
[14]S. D. Brorson, A. Kazeroonian, J. S. Moodera, D. W. Face, T. K. Cheng, E. P. Ippen, M. S. Dresselhaus, and G. Dresselhaus, Phys. Rev. Lett. **64**, 2172 (1990).
[15]M. Mihailidi, Q. Xing, K. M. Yoo, and R. R. Alfano, Phys. Rev. B **49**, 3207 (1994).
[16]W. S. Fann, R. Storz, H. W. K. Tom, and J. Bokor, Phys. Rev. Lett. **68**, 2834 (1992).
[17]W. S. Fann, R. Storz, H. W. K. Tom, and J. Bokor, Phys. Rev. B **46**, 13592 (1992).
[18]R. H. M. Groeneveld, R. Sprik, and A. Lagendijk, Phys. Rev. B **45**, 5079 (1992).
[19]C.-K. Sun, F. Vallée, L. Acioli, E. P. Ippen, and J. G. Fujimoto, Phys. Rev. B **48**, 12365 (1993).
[20]P. E. Hopkins, L. M. Phinney, and J. R. Serrano, J. Heat Transfer **133**, 044505 (2011).
[21]T. Q. Qiu and C. L. Tien, J. Heat Transfer **115**, 835 (1993).
[22]B. Y. Mueller and B. Rethfeld, Phys. Rev. B **87**, 035139 (2013).
[23]G. Tas and H. J. Maris, Phys. Rev. B **49**, 15046 (1994).
[24]R. H. M. Groeneveld, R. Sprik, and A. Lagendijk, Phys. Rev. B **51**, 11433 (1995).
[25]W. Wang and D. G. Cahill, Phys. Rev. Lett. **109**, 175503 (2012).
[26]D. G. Cahill, Rev. Sci. Instrum. **75**, 5119 (2004).
[27]P. E. Hopkins, J. R. Serrano, L. M. Phinney, S. P. Kearney, T. W. Grasser, and C. T. Harris, J. Heat Transfer **132**, 081302 (2010).
[28]A. J. Schmidt, X. Chen, and G. Chen, Rev. Sci. Instrum. **79**, 114902 (2008).
[29]J. K. Chen, W. P. Latham, and J. E. Beraun, J. Laser Appl. **17**, 63 (2005).
[30]R. Trebino, K. W. DeLong, D. N. Fittinghoff, J. N. Sweetser, M. A. Krumbgel, B. A. Richman, and D. J. Kane, Rev. Sci. Instrum. **68**, 3277 (1997).
[31]W. J. Scouler, Phys. Rev. Lett. **18**, 445 (1967).
[32]P. E. Hopkins, Appl. Phys. Lett. **96**, 041901 (2010).
[33]A. N. Smith and P. M. Norris, Appl. Phys. Lett. **78**, 1240 (2001).
[34]P. E. Hopkins, J. C. Duda, B. Kaehr, X. Wang Zhou, C.-Y. Peter Yang, and R. E. Jones, Appl. Phys. Lett. **103**, 211910 (2013).
[35]F. Abeles, *Advanced Optical Techniques*, edited by A. V. Heel (North-Holland Publishing Co., Amsterdam, 1967), pp. 145–188.
[36]J. Hohlfeld, S.-S. Wellershoff, J. Güdde, U. Conrad, V. Jähnke, and E. Matthias, Chem. Phys. **251**, 237 (2000).
[37]C. Kittel, *Introduction to Solid State Physics*, 6th ed. (John Wiley & Sons, Inc., New York, 1986).
[38]T. H. Geballe and W. F. Giauque, J. Am. Chem. Soc. **74**, 2368 (1952).
[39]L. Pietanza, G. Colonna, S. Longo, and M. Capitelli, Thin Solid Films **453–454**, 506 (2004).
[40]Z. Lin, L. V. Zhigilei, and V. Celli, Phys. Rev. B **77**, 075133 (2008).
[41]P. M. Norris, A. P. Caffrey, R. J. Stevens, J. M. Klopf, J. James, T. McLeskey, and A. N. Smith, Rev. Sci. Instrum. **74**, 400 (2003).
[42]M. I. Markovic and A. D. Rakic, Appl. Opt. **29**, 3479 (1990).
[43]R. E. Hummel, *Electronic Properties of Materials*, 3rd ed. (Springer-Verlag, New York, 2001).
[44]D. G. Cahill, P. V. Braun, G. Chen, D. R. Clarke, S. Fan, K. E. Goodson, P. Keblinski, W. P. King, G. D. Mahan, A. Majumdar, H. J. Maris, S. R. Phillpot, E. Pop, and L. Shi, Appl. Phys. Rev. **1**, 011305 (2014).
[45]M. Kaveh and N. Wiser, Adv. Phys. **33**, 257 (1984).
[46]X. Y. Wang, D. M. Riffe, Y.-S. Lee, and M. C. Downer, Phys. Rev. B **50**, 8016 (1994).
[47]C. Thomsen, H. T. Grahn, H. J. Maris, and J. Tauc, Phys. Rev. B **34**, 4129 (1986).
[48]D. Pines and P. Nozieres, *The Theory of Quantum Liquids* (Perseus, 1999).
[49]C.-K. Sun, F. Vallée, L. H. Acioli, E. P. Ippen, and J. G. Fujimoto, Phys. Rev. B **50**, 15337 (1994).
[50]M. L. Huberman and A. W. Overhauser, Phys. Rev. B **50**, 2865 (1994).
[51]A. V. Sergeev, Phys. Rev. B **58**, R10199 (1998).
[52]L. Guo, S. L. Hodson, T. S. Fisher, and X. Xu, J. Heat Transfer **134**, 042402 (2012).
[53]A. Giri, B. M. Foley, and P. E. Hopkins, J. Heat Transfer **136**, 092401 (2014).